INTERNATIONAL JOURNAL OF CLIMATOLOGY
Int. J. Climatol. (2014)
Published online in Wiley Online Library
(wileyonlinelibrary.com) DOI: 10.1002/joc.3948

The changing characteristics of monsoon rainfall in India during 1971–2005 and links with large scale circulation

Dileep K. Panda* and A. Kumar

Directorate of Water Management (ICAR), Chandrasekharpur, Bhubaneswar, Odisha, India

ABSTRACT: This study examines the changes in monsoon rainfall of India using a suite of extreme indices defined by the Expert Team on Climate Change Detection Monitoring and Indices (ETCCDMI) to make the Indian results comparable internationally, in addition to the use of some relevant indices particularly developed for the Indian climate. To this end, the recently developed high resolution daily gridded ($0.5^\circ \times 0.5^\circ$) rainfall dataset for the period 1971–2005 has been analysed using robust nonparametric techniques. Despite the high interannual variability and spatial diversity of the Indian climatology, the results reveal signal of changes for several extreme rainfall indices, generally consistent with the simulated outcome of an intensified Indian monsoon rainfall in the context of global warming. A predominant decrease in wet days, moderate and total rainfall is observed in the high rainfall regions of northeast, central and southwest India. In the active monsoon months of July and August, the dry spells defined by the maximum length of consecutive dry days (CDD) have increased significantly over the north and central regions of India, suggesting a serious threat to the Indian agriculture. Simultaneously, the extreme rainfall indices, based on the percentile and absolute values, show increasing trends over large parts of the country. The probability density function (PDF) of several indices show noticeable changes since the 1990s over the homogeneous central and northeast parts of India. The indices representing the total monsoon rainfall and dry spells are better correlated with the El Niño–Southern Oscillation (NINO3.4), compared to that of the Indian Ocean Dipole Mode Index (IODMI). The mapping of the observed rainfall trends and their correspondence to the large scale circulation modes is expected to assist the policy makers to prioritize the mitigation and adaptation strategies.

KEY WORDS Indian monsoon rainfall; global warming; climate variability; extreme rainfall indices; trend analysis

Received 30 January 2013; Revised 18 November 2013; Accepted 13 January 2014

1. Introduction

Examining the changes in mean and extreme climatic states has become a focused research theme because of the serious economic and environmental impacts of the recent extreme events in different parts of the world. Several studies have been carried out at the global scale (Frich *et al.*, 2002; Kiktev *et al.*, 2003; Alexander *et al.*, 2006), country-specific and cross-country domains (Klein Tank and Können, 2003; Vincent and Mekis, 2006; Griffiths and Bradley, 2007) to formulate sustainable development and adaptable strategies. Most of these studies have used the extreme climate change indices defined by the Expert Team on Climate Change Detection Monitoring and Indices (ETCCDMI, http://cccma.seos.uvic.ca/ETCCDMI/), a joint venture of the World Meteorological Organization Commission for Climatology (CCI) and the World Climate Research Program Climate Variability and Predictability (CLIVAR). The results of these studies suggest that the increasing extreme rainfall events are a consequence of the increased atmospheric moisture content associated with global warming. However, the signal of change is spatially less consistent for rainfall extremes in contrast to an apparent change in temperature extremes.

In general, there has been little research into the changes in extreme indices of the Asian summer monsoon rainfall, primarily because of the lack of high-resolution daily dataset (Frich *et al.*, 2002), although the monsoon rainfall sustains two-thirds of the world's population and also defines essential features of the earth's climate (Webster *et al.*, 1998). For the Indian subcontinent, a little change in distribution of the summer monsoon rainfall (June to September) directly affects the human society and natural systems since nearly 68% of over 1 billion population of the country depends on monsoon sensitive agriculture and allied sectors for their livelihood. For example, a deficit of only 19% monsoon rainfall in 2002 led to an estimated loss of billions of dollars (Gadgil *et al.*, 2003). In recent years, occurrence of heavy downpour evacuates millions people and damages the infrastructure particularly in the densely populated low-lying areas along the 5423 km mainland coast line. A record extreme rainfall event of 944 mm day^{-1} (i.e. on 26 July 2005) in Mumbai led to considerable loss of property and human lives.

* Correspondence to: D. K. Panda, Directorate of Water Management (ICAR), Chandrasekharpur, Bhubaneswar 751023, Odisha, India.
E-mail: dileeppanda@rediffmail.com

© 2014 Royal Meteorological Society

Given the large spatial and temporal variability of monsoon rainfall in India, literature pertaining to the extreme rainfall analysis is limited. For the period 1910–2000, Sen Roy and Balling (2004) observed increases in the frequency of extreme rainfall events in the northwestern and southern peninsular region of India. In central India, intense rainfall events showed increasing trends along with decreases in moderate rainfall events for the period 1951–2000 (Goswami *et al.*, 2006). During the last century, Rajeevan *et al.* (2008) reported that the inter-decadal variation in frequency of extreme rainfall has experienced marked decreases during the 1940s and 1950s, consistent with the cooling phase of the tropical sea surface temperature (SST). Krishnamurthy *et al.* (2009) observed that the northern and central regions of India have experienced a decreasing trend in the frequency and intensity of rainfall in contrast to an increasing trend in the coastal regions of the peninsula India for the period 1951–2003. For the same period, however, the study of Kishtawal *et al.* (2009) indicated that the urban regions of India have experienced an increasing trend in the frequency of extreme rainfall events. In contrast, for the period 1975–2006, the extreme rain events have decreased significantly in northeast India (Goswami *et al.*, 2010). Recently, Ghosh *et al.* (2012) observed an increasing spatial variability in extreme rainfall accompanied by a lack of uniformity in trends. It can be stated from the results of the studies illustrated above that the Indian monsoon rainfall trends are sensitive to the definition of extreme indices, record length, density and spatial dimension of the dataset used for the analysis. The lack of consensus in terms of the space-time disparity in trend results and their attribution in the recent studies, as highlighted by Ghosh *et al.* (2012), is the key motivation to further investigate the extreme rainfall characteristics using a variety of indices and high resolution datasets to precisely capture the regional variability.

The broad objective of this study is to investigate the possible changes in mean and extreme monsoon rainfall characteristics in India, using the indices developed by the ETCCDMI along with the indices relevant to the Indian climate. To this end, the recently updated high resolution gridded ($0.5^\circ \times 0.5^\circ$) daily rainfall dataset for the period 1971–2005 (Rajeevan and Bhate, 2009) is analysed using robust statistical tools. Although ETCCDMI has developed a suite of indices using a consistent methodology to evaluate and compare the changes in extreme rainfall internationally, till date no national study has been undertaken for the Indian subcontinent. Klein Tank *et al.* (2006) examined the linear trends in annual extreme rainfall of the central and south Asia, using some of the ETCCDMI indices, which showed no consistent pattern of change. Keeping in view the economic and hydrological impacts of monsoon rainfall, they underscored the need of assessing the changes in extreme indices of the monsoon season employing a more advanced robust trend estimates instead of the previously used outlier-sensitive linear regression method.

Several research papers have shown that a noticeable transition (shift) in atmospheric variables has occurred since the early 1970s (Bainnes and Folland, 2007; Carvalho *et al.*, 2010), which correspond to the most warming period of the last century (Houghton *et al.*, 2001). In particular, for the tropical and subtropical regions, rainfall has decreased along with increases in intensity of tropical cyclone and storm, leading to increases in land areas affected by droughts since the 1970 (Trenberth *et al.*, 2007; Klein Tank *et al.*, 2009). It is, therefore, of scientific and social interest to investigate the changes in different aspects of rainfall characteristics during the post-transition global warming era. This is to ascertain whether there has been any systematic change, and to validate the predicted warming induced intensification of the Indian monsoon rainfall (Kumar *et al.*, 2006; May, 2011). Naidu *et al.* (2009) studied the monthly rainfall trends of 30 meteorological subdivisions of India during the warming era. However, examining the changes in extreme indices can provide strong signals of climate change, as an intensified hydrological cycle would result in more extreme rainfall events (Folland *et al.*, 2001).

It is also well known that the large scale circulation modes, the El Niño-Southern Oscillation (ENSO) and the Indian Ocean Dipole (IOD), play an important role in modulating the interannual variability of monsoon rainfall (Krishna Kumar *et al.*, 1999; Ashok *et al.*, 2001). In addition, the tropical Atlantic SST is also correlated with the monsoon rainfall variability (Kucharski *et al.*, 2009). As several characteristics of ENSO and its relationship with the IOD events has changed since the 1970s (Annamalai *et al.*, 2005), assessing the relative influence on rainfall indices in this study will improve the understanding and predictability during the post-transition period. Finally, the trend magnitudes are interpolated, so that the spatial differentiation of the changes could be clearly assessed to formulate the disaster management policy. The paper is organized as follow. In Section 2, we describe the datasets and extreme rainfall indices. The trend results of rainfall indices are presented in Section 3. Section 4 explains the relationships with ENSO and IOD indices. This study is completed with a detailed discussion and conclusion in Section 5.

2. Dataset and methods

2.1. Dataset and indices

This study used the recently updated gridded dataset of daily monsoon rainfall of 1240 grids at the spatial resolution of $0.5^\circ \times 0.5^\circ$ for the period 1971–2005 (Rajeevan and Bhate, 2009), which represents uniformly the diverse climate of India (Figure 1). This dataset was developed by the Indian Meteorological Department (IMD) particularly for mesoscale meteorological applications using quality controlled rainfall data from more than 3000 rain gauge station spread over India. Location of the rain gauge stations considered for developing the gridded rainfall dataset and the quality control measures are described in

© 2014 Royal Meteorological Society

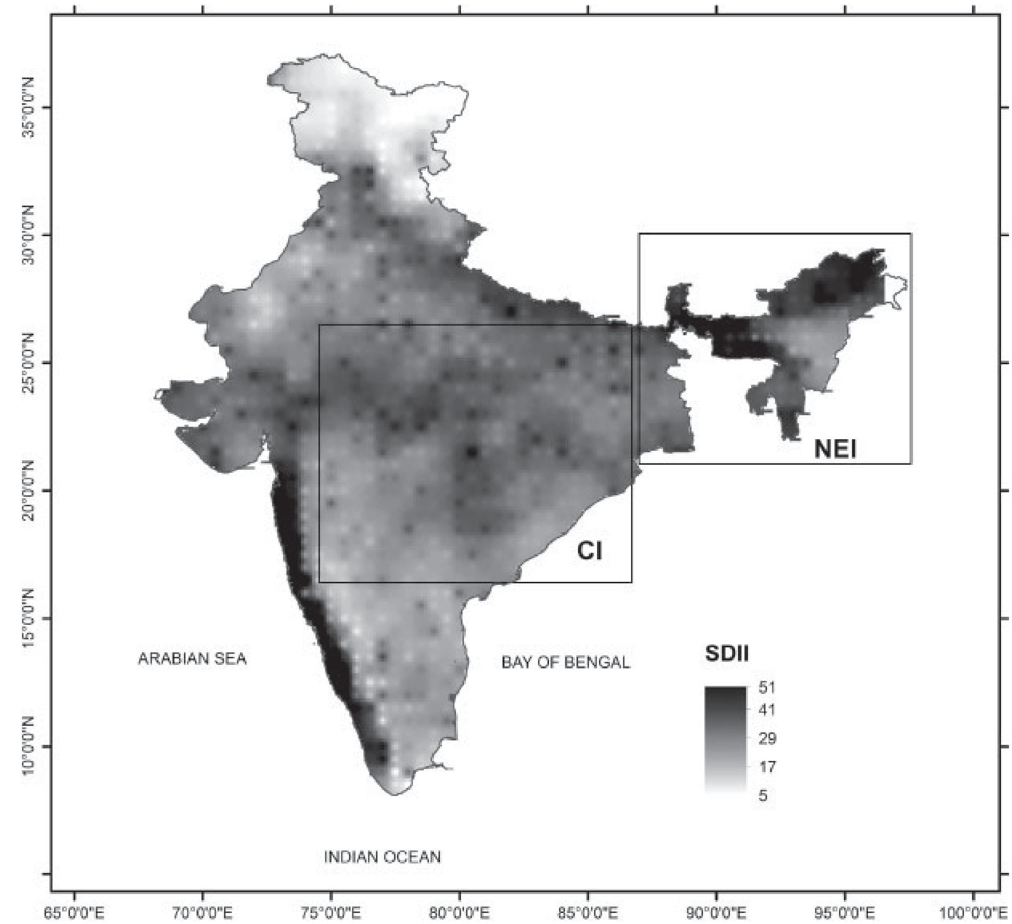

Figure 1. Schematic map of the Indian subcontinent shows the spatial distribution of simple daily intensity index (SDII, mm per day), indicating a high variability of the average precipitation on wet days (rainfall ≥ 1 mm) in the monsoon season (June to September). The central India (CI), which is influenced by the depression induced rainfall over the Bay of Bengal, and the high rainfall region of northeast India (NEI) are demarcated by the boxes.

detail by Rajeevan and Bhate (2009). This $0.5^\circ \times 0.5^\circ$ resolution dataset is highly and significantly correlated with APHRODITE dataset of Asia, and has been used for trend analysis (Yatagai *et al.*, 2012; Das *et al.*, 2013; Duncan *et al.*, 2013), thus suggesting the temporal homogeneity. In addition, this dataset has been used for validation of the model-derived rainfall over the Indian subcontinent, showing consistent spatio-temporal rainfall patterns (Pattnayak *et al.*, 2013; Srinivas *et al.*, 2013). Table 1 presents the rainfall indices, illustrating different aspects of total rainfall and dry and wet extremes in terms of intensity, frequency and magnitude. The extreme rainfall indices based on the count of days over a fixed threshold are necessary for the impact assessment and regional planning, whereas the percentile-based indices are pertinent for the climate change detection studies over diverse ecosystems (Haylock and Nicholls, 2000; Klein Tank and Können, 2003).

Although most of the indices were calculated using the daily gridded data of the monsoon season based on the ETCCDMI definition (Klein Tank *et al.*, 2009), the indices relevant to reflect the extremes of the Indian climate were also included. To make the calculation of indices consistent, a wet day is defined when rainfall ≥ 1 mm and a dry day when rainfall < 1 mm, although IMD defines a rainy day when rainfall ≥ 2.5 mm. The total monsoon rainfall on wet days (PRCPTOT) and the average wet day rainfall intensity (SDII) are indicative of the changes in entire monsoon rainfall. It is necessary to study the changes in moderate rainfall (RM), as it sustains the Indian agriculture and coastal ecosystems contributing about 85% of the total monsoon rainfall. More important, however, is the study of drought indices, such as the maximum number of consecutive dry days (CDD) and the aridity intensity index (AII), since they directly affect the predominant monsoon dependent agriculture at its critical stages of growth. While the CDD index characterizes the longest dry spell, the AII index reflects the magnitude of dryness in terms of moisture availability for crop production. As the AII index uses below 10 mm rainfall threshold to define a dry day, decreases in AII indicates a moisture stress scenario from agriculture prospective (Costa and Soares, 2009).

The maximum 1-day (RX1D) rainfall index is an important indicator because of its social and environmental impacts. Moreover, the heavy rainfall index, defined by the rainfall events over 100 mm (R100), is a relevant

© 2014 Royal Meteorological Society

Table 1. Extreme rainfall indices based on the ETCCDMI and the Indian definitions with their units. A wet day is defined when the daily rainfall amount (RR) ≥ 1 mm and a dry day when RR < 1 mm. All the indices are calculated for the monsoon season (June to September).

Index	Definition	Unit
PRCPTOT	Total monsoon rainfall (precipitation) on wet days	mm
SDII	Simple daily intensity index. Average precipitation on wet days	mm
RM	Moderate precipitation days for the Indian scenario. Monsoon count of days when 5 mm ≤ RR < 100 mm.	days
CDD	Consecutive dry days. Maximum number of consecutive dry days	days
AII	Aridity intensity index. Average precipitation on dry days, which is the ratio between the total rain on dry days and the number of dry days. Here, a dry day is defined as RR < 10 mm	days
RX1D	Maximum 1-day precipitation	mm
R100	Heavy precipitation days for the Indian scenario. Monsoon count of days when RR ≥ 100 mm	days
R95P (R99P)	Fraction of monsoon total precipitation (i.e. PRCPTOT) contributed from very heavy wet days, which is the ratio of total monsoon precipitation when RR > 95th percentile (99th percentile) of 1971–1990 daily rainfall on wet days to the monsoon total during the entire period	%
RF95P (RF99P)	Frequency of exceedance for the 95th percentile (99th percentile) threshold. For each grid cell, the 95th and 99th percentiles of the daily monsoon rainfall on wet days were calculated for each year and the median value of these percentiles across the study period was treated as the threshold value for calculating the extremes. Frequency of exceedance for grid j and year t is given by $F_{jt} = \sum_{i=1}^{122} S_{RR_{itj} > RR_j*}$ where RR_{itj} is the monsoon rainfall on day i in year t at grid j, RR_j^* is the threshold rainfall for grid j, S takes the value 1 if $R_{itj} > R_j^*$ and 0 otherwise	days
RI95P (RI99P)	Intensity of exceedance for the 95th percentile (99th percentile) threshold. For grid j and year t, the intensity of rainfall exceedance is calculated as $I_{jt} = \left(\frac{\sum_{i=1}^{122} S_{RR_{itj} > RR_j*} RR_{ijt}}{F_{jt}} \right) S_{F_{jt>0}}$	mm

measure for the Indian climatology in terms of extensive damage to life and property, compared to the ETCCDMI defined heavy and very heavy rainfall indices (i.e. R10 and R20). The indices reflecting the magnitudes of extreme rainfall (R95p and R99p) evaluates the fraction of total monsoon rainfall contributed from very heavy wet days above the 95th and 99th percentile based on the percentile of the 1971–1990 period daily rainfall data. Instead of the fixed thresholds, the frequency of extreme rainfall, such as the RF95p and RF99p indices, are based on the varying thresholds for different grids to capture the diverse climate of India (Krishnamurthy *et al.*, 2009). Furthermore, analysis of the intensity of rainfall using the RI95p and RI99p indices, which fundamentally differs from the R95p and R99p indices in terms of percentile calculation, will improve the understanding of changes in extreme magnitude. Most of the extreme climatic events have occurred since the 1990s in India as well as in other parts of the world, and therefore, the pre-1990 period is used as the base period to calculate the ETCCDMI extreme indices. To compare the recent changes in the monsoon rainfall indices, we assessed the probability density function (PDF) for the pre-1990 (1971–1989) and post-1990 (1990–2005) periods using all the grids over the homogeneous central and northeast parts of India (Figure 1).

To associate the variability in rainfall indices with the large-scale climatic modes, the recently developed NOAA Extended Reconstructed Sea Surface Temperature Version 3 (ERSST.v3b) dataset at a spatial resolution of $2^\circ \times 2^\circ$ was used (Smith *et al.*, 2008). In this study, NINO3.4 and the Indian Ocean Dipole Mode Index (IODMI) represent the ENSO and IOD, respectively. The NINO3.4 index was derived from the SST anomalies of ERSST.v3b dataset by averaging over the Niño 3.4 region (5°N–5°S, 120°W–170°W). Similarly, the IODMI was calculated from the same dataset by taking the difference of SST anomalies between the western (50°E–70°E, 10°S–10°N) and eastern (90°E–110°E, 10°S-equator) tropical Indian Ocean (Saji *et al.*, 1999). Both the indices have been normalized and averaged over the monsoon season. Most of the previous studies have investigated the influence of ENSO and IOD modes on the total monsoon rainfall (Sarkar *et al.*, 2004; Ashok and Saji, 2007). In this study, we explored whether there exists a similar or different relationship with a suite of rainfall indices, particularly during the warming era. We computed partial correlation and their significance ($\alpha = 0.05$) based on

© 2014 Royal Meteorological Society

the two tailed Student t-test to address the influence of multiple drivers on each of the considered rainfall indices (Ashok *et al.*, 2004; Taschetto *et al.*, 2011). To understand the regional influence, the interpolated values of the correlation coefficients have been mapped.

2.2. Trend test

Since extreme indices generally follow the non-Gaussian distribution, the nonparametric Mann–Kendall test was used to detect the monotone trends in extreme rainfall indices at each grid. This rank-based test, which makes no assumption about the underlying probability distribution of data or linearity of trend and also robust to the effect of outliers in extreme indices, has been used widely in literature to assess trends in hydroclimatic time series (Lettenmaier *et al.*, 1994; Hisdal *et al.*, 2001; Zhang *et al.*, 2001). The test statistics is given by

$$S = \sum_{i=1}^{n-1} \sum_{j=i+1}^{n} \operatorname{sgn}\left(X_j - X_i\right), \text{for all } 1 \le i < j \le n \quad (1)$$

where X_i and X_j are the sequential data values from the sample of n independently and identically distributed random variables; sgn() is the sign function, which is equal to 1,0,−1 depending on whether the difference $(X_j - X_i)$ is positive, zero or negative. Even for a small sample size $n \ge 10$, the statistics S is approximately normally distributed with the mean and the variance given by

$$\mathrm{E}(S) = 0 \quad (2)$$

and

$$\operatorname{var}(S) = \frac{1}{18}\left(n\,(n-1)\,(2n+5) - \sum_{l=1}^{m} t_l\,(t_l-1)\,(2t_l+5)\right) \quad (3)$$

where m is the number of tied ranks groups, each with t_l tied observations. The standardized test statistics Z is given by

$$Z = \frac{S - \delta}{\sqrt{\operatorname{var}(S)}} \quad (4)$$

where δ is equal to 1,0,−1 depending on whether S is positive, zero, or negative. Under the null hypothesis of no trend, the standardized test statistic Z follows the standard normal distribution with mean zero and variance one. Using a two tailed test procedure, if $|Z| > Z_{1-\alpha/2}$, the null hypothesis is rejected at significance level α. As recommended by Nicholls (2001), the statistical significance the trend has been assessed at the levels $\alpha = 0.05$, 0.1 and 0.2. However, the results and discussions are based on the mapping of the significant trends at the level $\alpha = 0.1$.

In spite of the robustness of the Mann–Kendall test to the distribution and idiosyncrasies of data, presence of positive (negative) serial correlation in the time series increases (decreases) the probability of detecting trends when no trend exist actually (Zhang *et al.*, 2001). Therefore, the test statistics was adjusted by determining the effective sample size (ESS) with the assumption that the underlying data follow a first order autoregressive process (Katz, 1985; Yue and Wang, 2002). The Mann–Kendall test does not quantify the trend magnitude. The robust Kendall slope (β) was used to assess the slope of the monotone trend (Sen, 1968; Hirsch *et al.*, 1982). The test statistic is given by

$$\beta = \operatorname{median}\left(\frac{X_j - X_i}{j - i}\right) \quad (5)$$

A positive S corresponds a positive β and a negative S corresponds a negative β, indicating the increasing and decreasing trend, respectively. The inverse distance weighted (IDW) method (Hartkamp *et al.*, 1999) was used to interpolate the trend magnitudes.

3. Results

3.1. Changes in total rainfall indices

Tables 2–4 present a summary of the trend analysis. It can be seen that the proportion of trends differ with respect to the indices and the percentile thresholds, representing even the same rainfall characteristics. The identification of a large number of nonsignificant trends is due to the obvious reason of a large interannual variability in terms of the deficit and excess rainfall years during the study period; the country has experienced seven below normal drought (dry) years (i.e. 1972, 1979, 1982,

Table 2. Frequency of the increasing and decreasing trends in indices representing the total monsoon rainfall (PRCPTOT, Wet days, SDII, RM), and their significance at the $\alpha = 0.05$, 0.1 and 0.2 levels from the total of 1240 grids

Indices	Total		$\alpha = 0.05$		$\alpha = 0.1$		$\alpha = 0.2$	
	Increasing	Decreasing	Increasing	Decreasing	Increasing	Decreasing	Increasing	Decreasing
PRCPTOT	569	651	39	58	69	111	125	168
Wet days	483	745	53	84	86	166	157	277
Wet days (June)	682	535	54	23	99	48	187	97
Wet days (July)	462	760	33	65	58	118	106	218
Wet days (August)	446	779	36	101	66	185	107	305
Wet days (September)	578	633	28	20	69	48	119	117
SDII	646	566	69	64	124	102	227	168
RM	508	715	47	64	81	131	131	240
RM (July)	507	717	25	38	56	102	103	195
RM (August)	459	768	30	86	67	175	115	292

© 2014 Royal Meteorological Society

Table 3. Frequency of the increasing and decreasing trends in the extreme dry indices (CDD, AII), and their significance at the $\alpha = 0.05$, 0.1 and 0.2 levels from the total of 1240 grids.

Indices	Total		$\alpha = 0.05$		$\alpha = 0.1$		$\alpha = 0.2$	
	Increasing	Decreasing	Increasing	Decreasing	Increasing	Decreasing	Increasing	Decreasing
CDD	565	655	28	50	76	96	138	162
CDD (June)	471	751	16	32	37	90	72	183
CDD (July)	692	537	31	19	77	43	157	95
CDD (August)	708	501	97	95	222	162	382	267
CDD (September)	248	925	2	39	16	98	40	222
AII	490	734	48	87	89	174	159	266
AII (June)	644	573	45	30	88	57	190	123
AII (July)	473	746	30	67	54	128	103	243
AII (August)	474	746	36	78	71	157	126	263
AII (September)	646	568	33	28	70	54	130	118

Table 4. Frequency of the increasing and decreasing trends in the absolute and percentile-based extreme wet indices (RX1D, R100, R95p, R99p, RF95p, RF99p, RI95p, RI99p), and their significance at the $\alpha = 0.05$, 0.1 and 0.2 levels from the total of 1240 grids.

Indices	Total		$\alpha = 0.05$		$\alpha = 0.1$		$\alpha = 0.2$	
	Increasing	Decreasing	Increasing	Decreasing	Increasing	Decreasing	Increasing	Decreasing
RX1D	731	492	61	39	106	63	211	118
R100	696	447	10	7	34	19	78	48
R95p	741	479	79	32	147	68	243	121
R99p	775	450	35	5	81	16	157	51
RF95p	676	550	45	45	99	80	196	149
RF99p	729	499	29	17	80	49	162	98
RI95p	710	515	57	38	118	70	219	104
RI99p	735	495	36	23	69	44	172	90

1986, 1987, 2002, 2004) and five above normal flood (wet) years (i.e. 1975, 1983, 1988, 1994, 2005), in addition to the frequent occurrence of regional scale rainfall anomalies. These, along with the diverse heterogeneity in rainfall distribution (Figure 1), possess difficulty in identifying consistent trends at the national or regional scale.

The monsoon rainfall total, PRCPTOT, exhibits a marginal dominance of the decreasing trends (Table 2), with the congregation of the significant downward trends in the central, peninsular (below the central India in Figure 1) and northeast regions of India, and the significant upward trends in the northern and central parts (Figure 2). This opposite spatial pattern in PRCPTOT could be due to the existing natural contradictions in rainfall anomalies in different parts of the country, as Krishnamurthy and Shukla (2000) observed that the anomaly of a particular pattern is observed in central India, while the anomaly of opposite pattern prevails over the foothills of the Himalayas and the southeastern peninsular India. It should be noted that the frequency of wet days in the monsoon season have decreased in high proportion, specially driven by the decreases in the active monsoon months of July and August (Table 2). The moderate rainfall events (RM), defined by the number of days with rainfall between 5 and 100 mm, have decreased in similar proportions to that of the wet days frequency at the seasonal and subseasonal scale. It is noteworthy to mention that the high rainfall regions of the country (i.e. parts of central India and northeast India, and the southwest coastal belt through which the monsoon enters the subcontinent) have experienced marked decreases in PRCPTOT, wet days and moderate rainfall patterns (Figure 2), with the latter indices having a more consistent spatial coherence than that of the PRCPTOT index. Although, the average rainfall intensity index, SDII, shows the trend signs that are of almost equal proportion, comparatively more increasing trends are identified at the higher levels of significance. The spatial distribution of the significant trends indicates isolated patches of increases and decreases in SDII, without reflecting clearly the regional orientation of PRCPTOT and the wet day frequency from which the SDII index is derived.

Figure 3 illustrates the changes in PDF for the indices representing the total monsoon rainfall between the pre-1990 (1971–1989) and the post-1990 (1990–2005) periods in central India and northeast India. For PRCPTOT, a clear rise in the PDF peak for the period 1990–2005, particularly in central India along with a marginal change to the shift without any noticeable shifts in central and northeast India, implying an increase in the frequency of average rainfall in recent years. In contrast, the frequency of average rainfall intensity, SDII, has dropped, while the PDF have marginally moved to the right, suggesting increases in the lower and upper quintiles of rainfall intensity in the recent epoch. The PDFs of the wet days and moderate rainfall frequency (Figure 3(b) and (d))

© 2014 Royal Meteorological Society

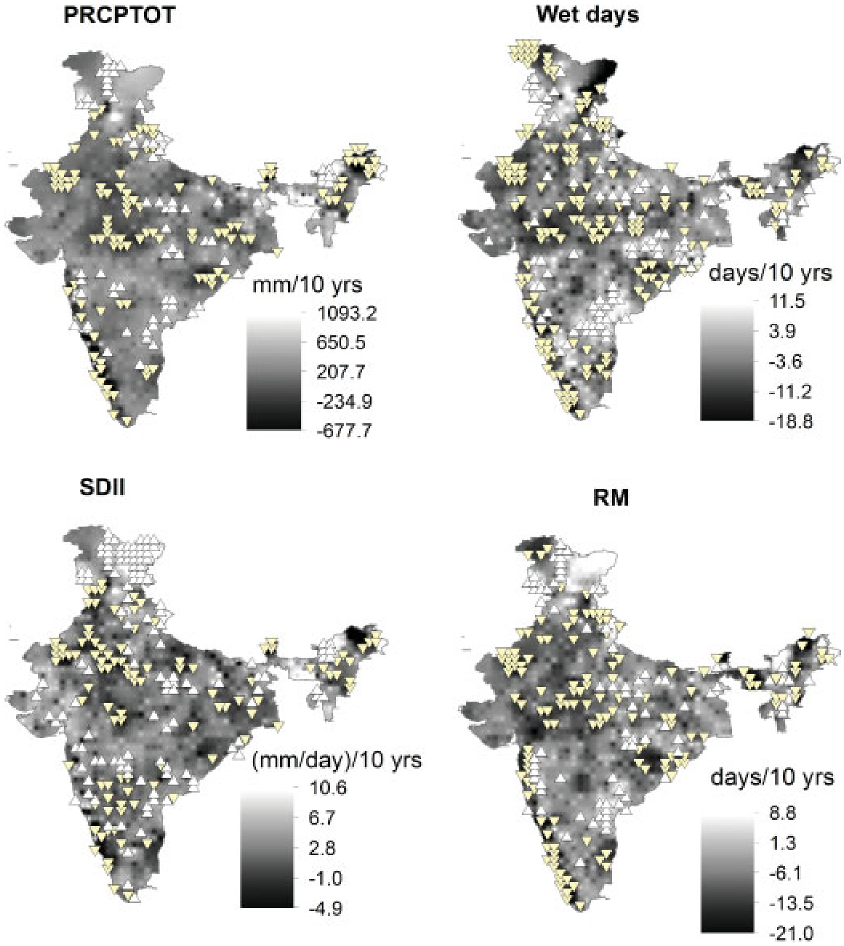

Figure 2. Spatial distribution of trends for total monsoon rainfall on wet days (PRCPTOT), wet days frequency with rainfall $\geq$ 1 mm, simple daily intensity index (SDII), and moderate rainfall with 5 mm $\leq$ rainfall $\leq$ 100 mm (RM) for the period 1971–2005. The significant ($\alpha = 0.1$) increasing and decreasing trends are denoted by upward and downward triangles, respectively. The interpolated values of the trend magnitudes are shown.

reflect more clear changes than that of the PRCPTOT and SDII indices (Figure 3(a) and (c)); the dominant feature of the recent period, irrespective of the regions, is the reduction in higher quintiles (i.e. the upper tail of the distribution), accompanied by an increase in the peak of the distribution. The recent period decrease in the wet day frequency in central India is more pronounced as evident from the PDF shift to the left for the period 1990–2005 (Figure 3(b)).

3.2. Changes in extreme dry indices

Table 3 presents the trends in CDD and AII, indicating the seasonal and subseasonal differences between and within the two drought indices. Increases in CDD reflect the rise in dry spells, while increases in AII suggest the rise in moisture availability. The most interesting feature to note is that the drought indices for the whole monsoon season have not captured the contradictory subseasonal patterns among the months June to September. This may be because of the reason that the rainfall distribution is not uniform throughout the four months (June to September) of the monsoon season, with the average rainfall of 169 mm (standard deviation: 28 mm) in June, 279 mm (standard deviation: 49 mm) in July, 249 mm (standard deviation: 30 mm) in August, 158 mm (standard deviation: 33 mm) in September, and 855 mm (standard deviation: 94 mm) in Monsoon season during the study period. In particular, while the increasing dry spell and moisture stress scenario in the active monsoon months of July and August is not reflected in the monsoon CDD, but captured to some extent in the monsoon AII index, the opposite tendency in the month of June and September is also confounded.

It is remarkable to note a distinct behaviour of CDD trends on a subseasonal scale (Table 3). For the monsoon onset month of June, the CDD index has decreased comparatively in northeastern parts of central India (not shown), representing the foothill region of the Himalayas (not shown). Although the elevated heat pump mechanism (Lau *et al.*, 2006), which brings warm and moist air from the adjacent Ocean and causes increased rainfall over north India in the pre-monsoon and early June period, could possibly explain the observed decreases in CDD and increases in wet days frequency, lack of observational support of the mechanism (Nigam and Bollasina, 2010) is also an issue that needs further investigation.

© 2014 Royal Meteorological Society

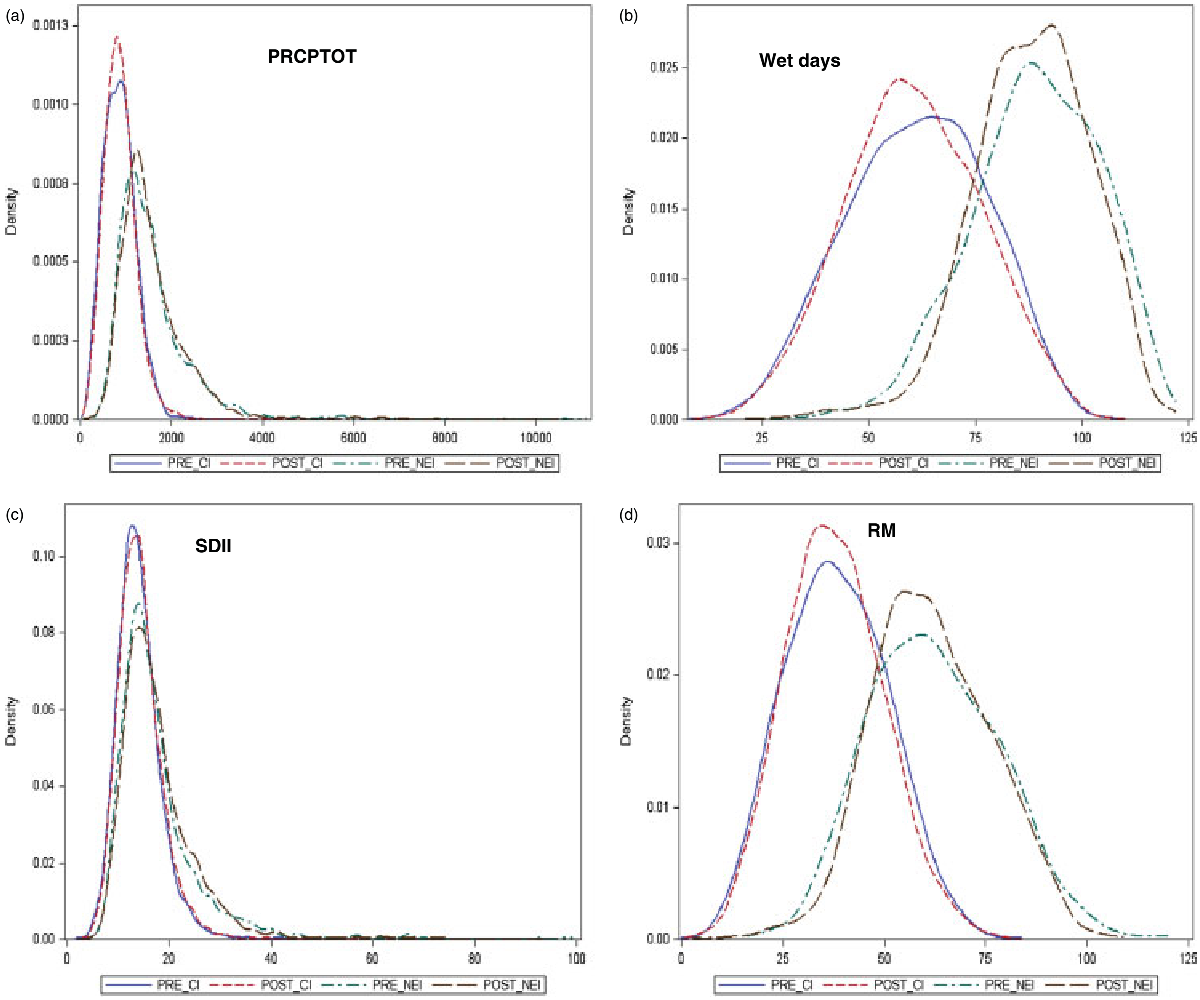

Figure 3. Probability density function (PDF) of (a) total monsoon rainfall on wet days (PRCPTOT), (b) wet days frequency with rainfall ≥ 1 mm, (c) simple daily intensity index (SDII), and (d) moderate rainfall with 5 mm ≤ rainfall < 100 mm (RM) for the pre-1990 period (1971–1989) in central India (PRE_CI) and northeast India (PRE_NEI) and for the post-1990 period (1990–2005) in central India (POST_CI) and northeast India (POST_NEI).

The most remarkable feature of the subseasonal results is the striking spatial gradient for both the CDD and AII indices in July and August (Figure 4). The observed dipolar distribution of trends in July and August suggests that the central and northern parts of India are vulnerable to drought, as evident from the predominance of the increasing (decreasing) trends in CDD (AII). The significant downward shift in depression frequency over the Bay of Bengal since 1971 (Panda *et al.*, 2013), which contributes a substantial amount of rainfall in central India, may have influenced in part the observed CDD and AII. In contrast, the southern parts of the country, except that of the southwest coastal tract, have experienced a wetting tendency during the study period. In the monsoon withdrawal month of September, decreases in the dry spells were observed in the northcentral parts and increases in eastern India (not shown). It should be pointed that the spatial distribution of the CDD and AII indices for the monsoon season did not show the distinct spatial coherence that we observe in the subseasonal scale, thus underscores the importance of the subseasonal analysis. The PDFs (Figure 5(b) and (c)) indicate that the drought spells in July have increased noticeably for the recent period (1990–2005) in central and northeast India, compared to the occurrence of both increasing and decreasing spells in August with no change in the peaks of the PDF. For the monsoon season as a whole, the occurrence of dry spells in the recent epoch is not captured in the PDF of CDD for both the regions (Figure 5(a)). For AII, however, the moisture stress in term of marked reductions in the upper and lower tails are compensated by the rise in the peak of the PDF (Figure 5(d)). A similar tendency is also observed in the July and August PDF of AII (not shown).

3.3. Changes in absolute and percentile-based extreme wet indices

For the maximum 1-day precipitation index, RX1D, relatively more grids have experienced an increasing trend (Table 4). While the significant increasing trends have scattered over the country with more congregation in south India (Figure 6), the northwestern and northeastern

© 2014 Royal Meteorological Society

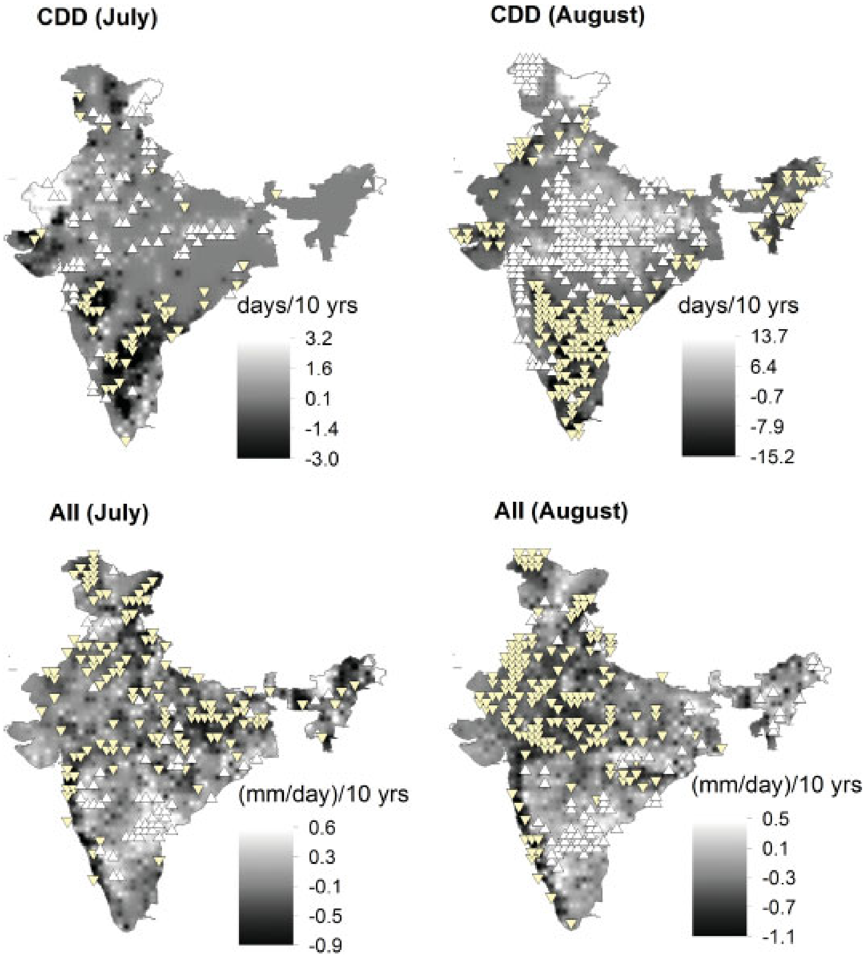

Figure 4. Spatial distribution of significant ($\alpha = 0.1$) trends for the maximum number of consecutive dry days (CDD) in July and August and aridity intensity index (AII) in July and August for the period 1971–2005. The increasing and decreasing trends are denoted by upward and downward triangles, respectively. The interpolated values of the trend magnitudes are shown.

parts have experienced most of the significant decreases. For the maximum 5-day precipitation, RX5D, both the increasing and decreasing trends along with their significance have occurred in equal proportion (not shown), suggesting a change in distribution of the extreme rainfall characteristic within a period of 5 days. Our result validate the prediction of the regional climate model PRECIS (Kumar *et al.*, 2006), showing a general increase in RX1D over the Western Ghat regions along the west coast and the northwestern peninsular India (below central India).

The heavy rainfall events above 100 mm, R100, show a marginal increase in its occurrence. It is, however, interesting to note that large number of grids show statistically nonsignificant trends because of the high interannual variability. Moreover, trend slope could not be quantified in most of the grids. At isolated locations, mostly in central and northeast India, few significant trends can be seen (Figure 6). Goswami *et al.* (2006) also observed no discernible trend in R100 from the individual station data due to the high interannual variability, and thus a sufficiently large area was considered to detect a common trend from the aggregated time series. The PDF of RX1D in central India shows a subtle shift in distribution to the right for the period 1990–2005 (Figure 7(a)), indicating more occurrences of the extremes in recent years. In contrast, occurrence of RX1D appears to have increased marginally in northeast India for the pre-1990 period. For R100, although no difference is seen in the PDF of the recent epoch compared to the pre-1990 period, the complex spatial and temporal evolution of R100 is evident from the skewed distributions (Figure 7(b)).

Table 4 shows that the magnitudes of extreme rainfall denoted by the fraction of total monsoon rainfall contributed from very heavy wet days above the 95th and 99th percentile, R95P and R99P, have comparatively higher proportion of increasing trends. However, the significant trends in R99P are less detected compared to R95P because of high interannual variability. Figure 6 indicates that the distribution of the significant trends in R95P does not show definite spatial pattern in spite of large areas being covered with the increasing trends. For R99P, however, the significant increasing trends are scattered over the country, except that of the northeast region where a mixture of opposite trends can be noted. The PDFs indicate that the distribution of R95P and R99P

© 2014 Royal Meteorological Society

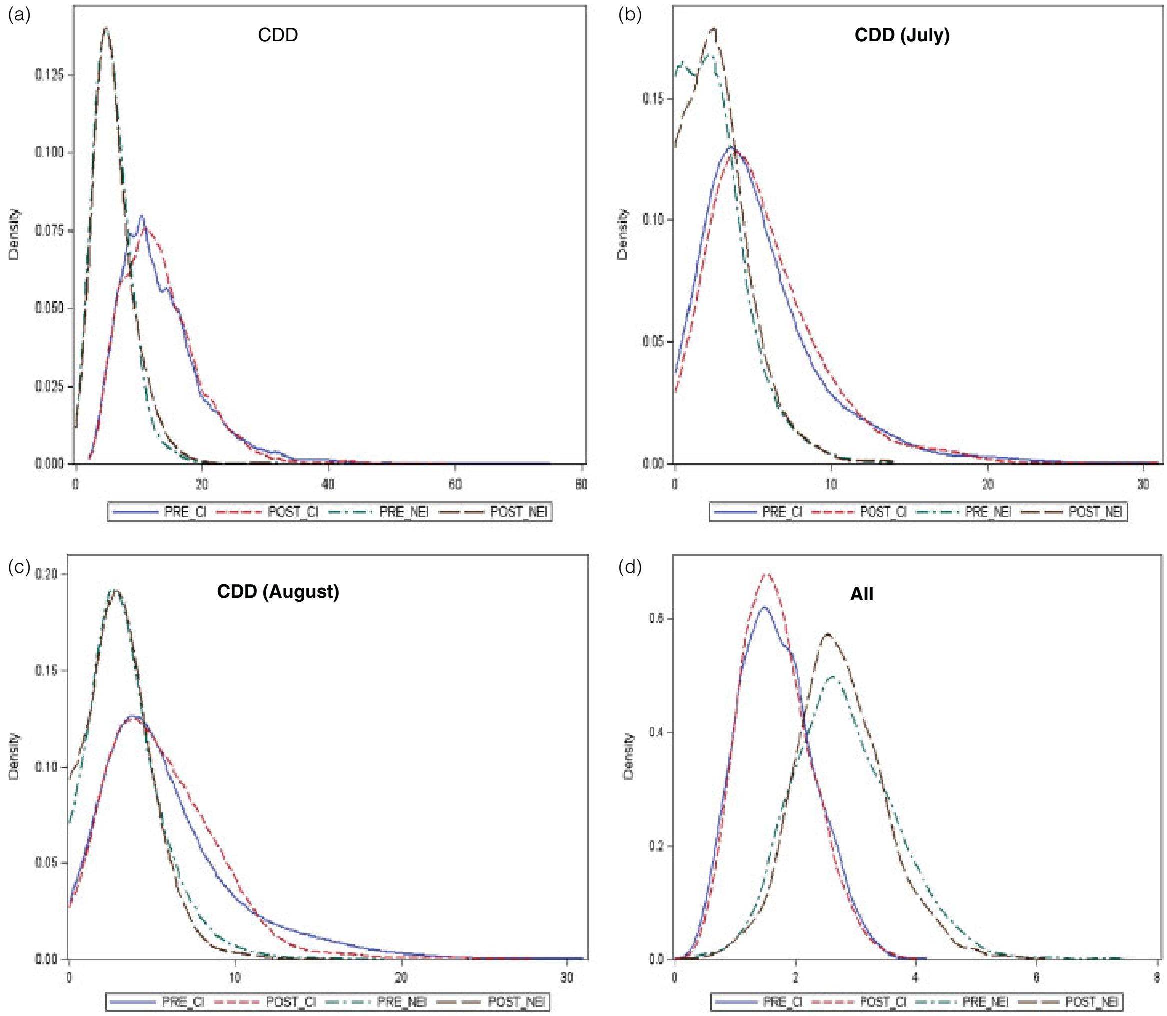

Figure 5. Probability density function (PDF) of (a) consecutive dry days (CDD) in the monsoon season, (b) CDD in July, (c) CDD in August, and (d) the monsoon aridity intensity index (AII) for the pre-1990 period (1971–1989) in central India (PRE_CI) and northeast India (PRE_NEI) and for the post-1990 period (1990-2005) in central India (POST_CI) and northeast India (POST_NEI).

has shifted towards an increased occurrence of extremes in central India since 1990s, while no perceptible change has occurred between the subperiods in northeast India (Figure 7(c) and (d)). It may be inferred that most of the increases in PRECPTOT and SDII in northern and central India (Figure 2) are due to the observed patterns in R95p and R99p.

The changes in exceedance frequency over the 95th and 99th percentile, RF95p and RF99P, show the more occurrences of the increasing trends (Table 4). For RF95P, the significant increasing and decreasing trends in RF95P have occurred simultaneously over large parts of the country, particularly prominent in central and northeast India (Figure 8). For RF99P, however, most of the spatial domain has experienced significant increases except the congregation of a few significant decreasing trends in northwest and northeast India. A similar distribution of trend frequency in the exceedance intensity of monsoon rainfall over the 95th and 99th percentile, RI95P and RI99P, suggests that not only the frequency but also the intensity of extreme rainfall has increased compared to the decreases (Table 4). The spatial distribution of the significant trends in RI95P and RI99P show a similar but spatially little more coherent pattern than that of the exceedance frequency (Figure 8). This difference may be due to the increase in intensity of rainfall events but not the frequency in some of the locations. The changes in the PDFs suggest that the intensity of rainfall in central India has increased marginally for the period 1991–2005 (Figure 9(c) and (d)), while the frequency of extreme rainfall show no perceptible difference between the subperiods (Figure 9(a) and (b)).

Using a dataset of 357 grids, Krishnamurthy *et al.* (2009) also observed a general increase in the frequency and intensity of monsoon rainfall, although the decreasing trends were noted in the central, northeastern and northern parts of India. Analysis of a high resolution dataset in this study, however, provides a coherent spatial pattern of changes applicable for implementing precautionary measures. What clearly stands out is that the southeast coastal region is highly vulnerable to both the frequency and intensity of extreme rainfall. It is

© 2014 Royal Meteorological Society

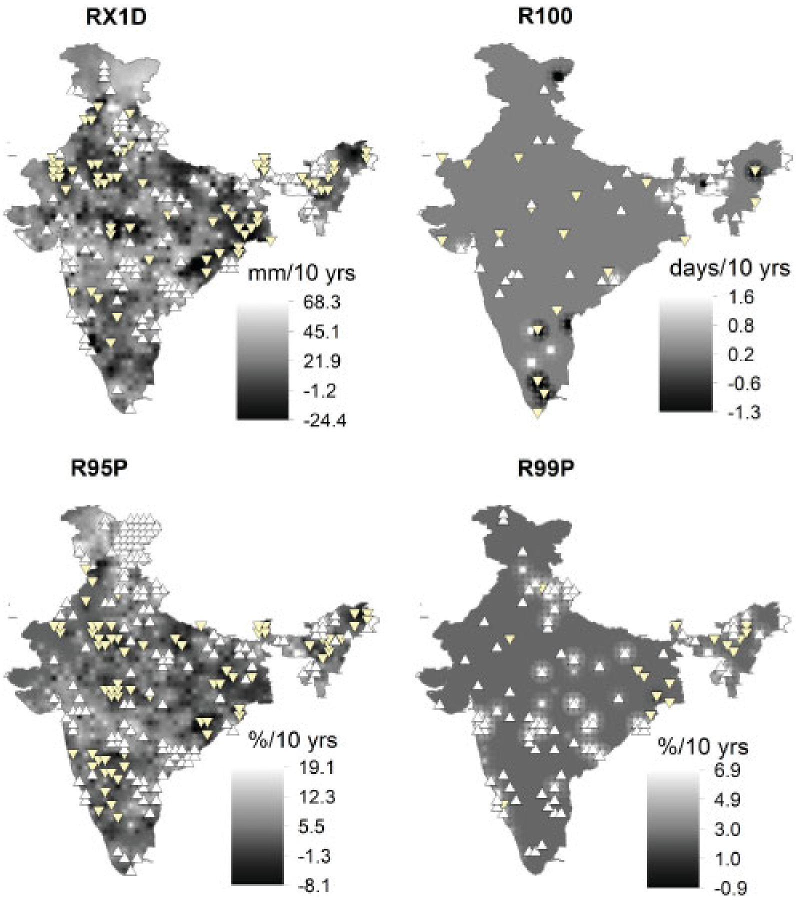

Figure 6. Spatial distribution of significant ($\alpha = 0.1$) trends for the maximum 1-day precipitation (RX1D), heavy rainfall events with rainfall ≥ 100 mm (R100), fraction of total monsoon rainfall contributed from very heavy wet days above the 95th percentile (R95P) and the 99th percentile (R99P) for the period 1971–2005. The increasing and decreasing trends are denoted by upward and downward triangles, respectively. The interpolated values of the trend magnitudes are shown.

also important to point out that the monsoon trough region, an area characterized by a low pressure feature that extends from southeast to northwest across the domain of central India, has experienced a mixture of increasing and decreasing trends as evident from most of the extreme indices described above.

4. Relations with ENSO and IOD indices

In general, occurrence of the El Niño event (warm phase) leads to deficit monsoon rainfall and vice versa for the La Niña event (cool phase). In addition, the positive (negative) IOD events results in excessive (deficit) monsoon rainfall. However, this relationship is governed by the relative influence of the phase and amplitude of both the indices as evident from the anomalous rainfall in India during the opposite phases of the ENSO and IOD modes (Figure 10). The normal or surplus rainfall in 1983, 1994, 1997 and 2003 is due to the positive IOD modes despite the presence of the simultaneous warm phase of the ENSO. But, the positive IOD has not diminished the influence of El Niño event in 1972, 1982 and 1987, leading to the occurrence of deficit rainfall. For this study period, the NINO3.4 has significant inverse relationship ($r = -0.37$) with the all India monsoon rainfall anomalies, while the IODMI shows a weak correlation ($r = -0.12$) (Figure 10). This result is similar to that obtained by Boschat *et al.* (2012) for the period 1979–2006. However, the linear relation differs at the regional and sub-seasonal scale. Table 5 presents the grid scale partial correlation of the ENSO and IOD indices with the rainfall indices (Ashok *et al.*, 2004; Taschetto *et al.*, 2011), illustrating the relationship between two variables by excluding the influence of the other independent variable (i.e. rainfall indices-NINO3.4/ SSTDMI and rainfall indices-IODMI/NINO3.4).

Consistent with the established negative (positive) relationship of ENSO (IOD) index with monsoon rainfall, Table 5 indicates that a high proportion of grids show a negative (positive) correlation between NINO3.4 (IODMI) and PRCPTOT, wet days and RM indices. The dryness index, CDD, is more frequently positively (negatively) correlated with the NINO3.4 (IODMI), and for the other drought index, AII, the relationship is opposite to that of CDD. However, the extreme wet indices exhibit a mixture of positive and negative correlation with the ENSO and IOD indices. Figure 11 presents the interpolated values of the correlation coefficients and the

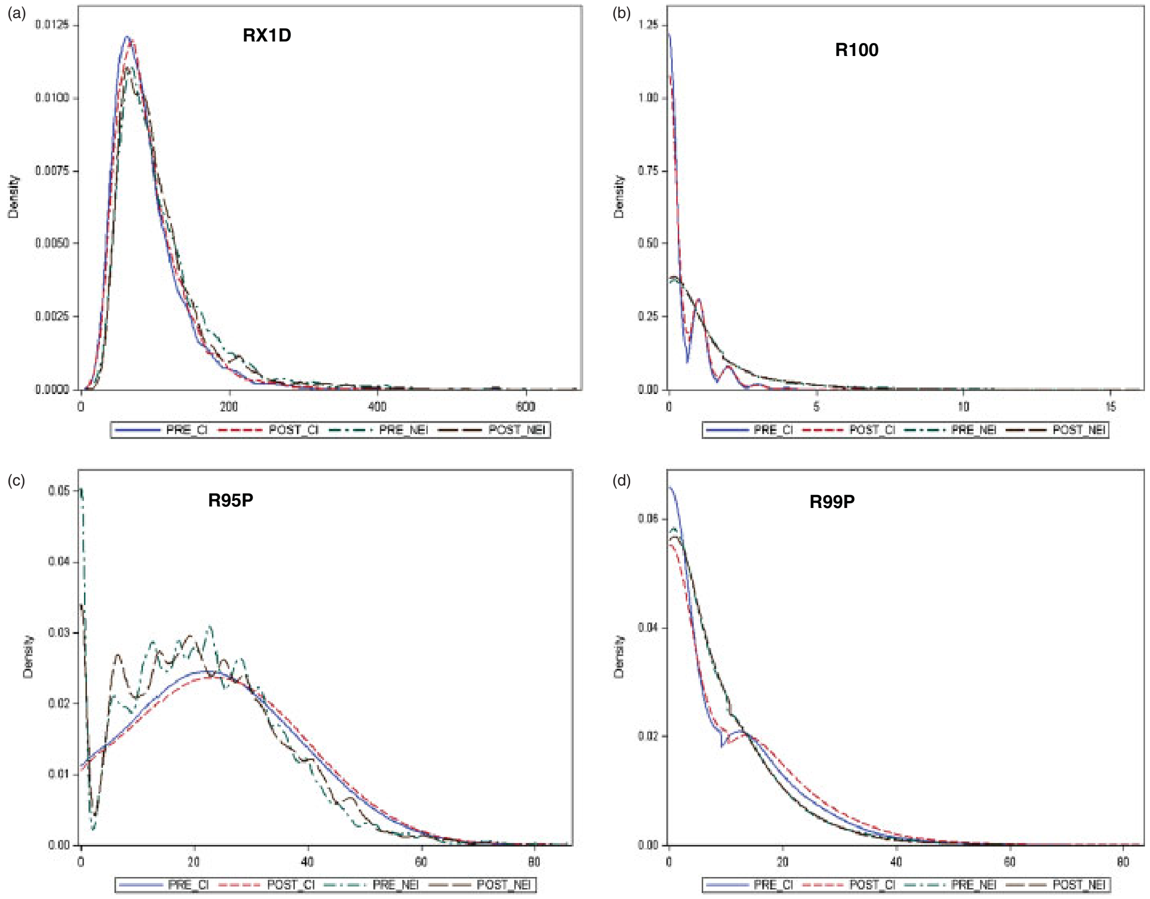

Figure 7. Probability density function (PDF) of (a) maximum 1-day precipitation (RX1D), (b) heavy rainfall events with rainfall $\geq$ 100 mm (R100), (c) fraction of total monsoon rainfall contributed from very heavy wet days above the 95th percentile (R95P) and (d) above the 99th percentile (R99P) for the pre-1990 period (1971–1989) in central India (PRE_CI) and northeast India (PRE_NEI) and for the post-1990 period (1990–2005) in central India (POST_CI) and northeast India (POST_NEI).

location of the significant ($\alpha = 0.05$) correlation coefficients, indicating the regionally coherent patterns. It is important to note a large scale influence of NINO3.4 on the indices representing the total rainfall and drought characteristics (i.e. PRCPTOT, wet days, SDII, RM, CDD and AII) (Figure 11(a)). This suggest that when the NINO3.4 index is positive (El Niño event), most parts of the country tend to have less monsoon rainfall because of the reduction in wet days and moderate rainfall events, but more of dry spells, and vice versa when the NINO3.4 is negative (La Niña event). The positive anomalies of the tropical Indian Ocean SST are generally associated with the El Niño events, leading to droughts through large scale subsistence (Goswami *et al.*, 2006). We find that the SST over the tropical Indian Ocean (Mean: 28.1 °C, standard deviation 0.2 °C) has increased significantly at the rate of 0.13 °C per decade for the period 1971–2005. Figure 8(b) also displays an increasing trend in NINO3.4, consistent with the large scale influence of the El Niño events on the observed drought vulnerability. However, the relationship of NINO3.4 with the wet extreme indices (i.e. RX1D, R100, R99p, RF99p and RI99p) is spatially less consistent, with the patches of positive and negative correlations congregated more in central India.

Although the IODMI index is linked to a lesser extent with the indices representing the total rainfall and drought spells as evident from the proportion of the significant correlation coefficients (Table 5), there is a spatial coherence that can be interpreted (Figure 11(b)). In particular, most of the significant positive correlation of IODMI with PRCPTOT, wet days, RM and AII are concentrated around the monsoon trough across central India. This is consistent with the finding of Behera *et al.* (1999) and Ashok *et al.* (2001), who inferred that the IOD events modulate the meridional circulation by inducing anomalous convergence (divergence) patterns over the Bay of Bengal during positive (negative) IOD phase, resulting in surplus (deficit) rainfall around the monsoon trough. However, the IOD index is negatively related with the total as well as some of the extreme rainfall indices in the peninsular region. In central India, the correspondence with the extreme indices is less clear. Ajayamohan and Rao (2008) reported that the recent IOD events have modulated the extreme rainfall (R100) in central India, as a significant correlation was observed between the eastern pole of IOD and the number of extreme rainfall events during the period 1982–2004. Consistent with this result, we also find a significant correlation ($\alpha = 0.05$) between

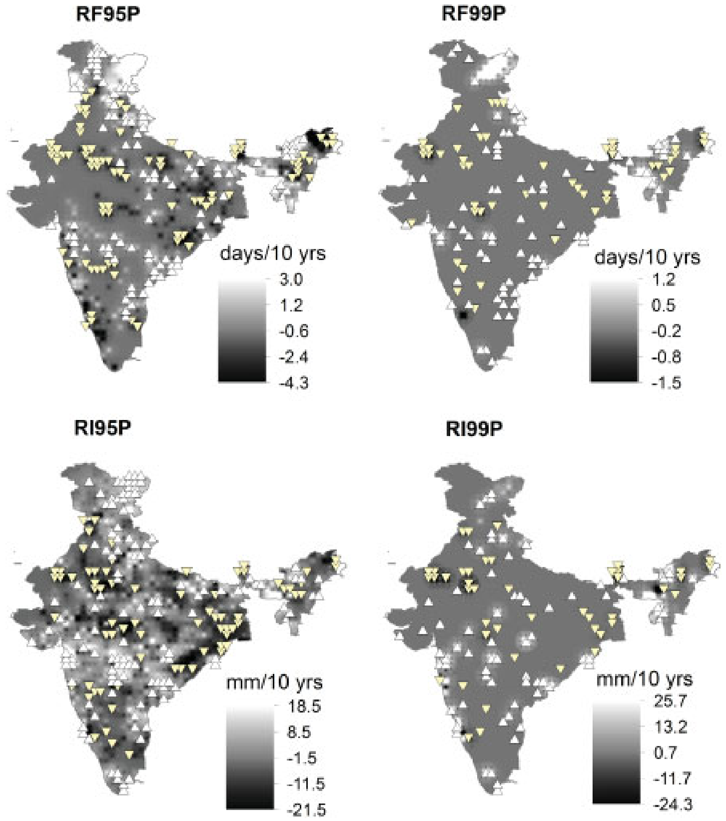

Figure 8. Spatial distribution of significant ($\alpha = 0.1$) trends for the frequency of exceedance of the 95th percentile (RF95P), 99th percentile (RF99P), and for the intensity of exceedance of the 95th percentile (RI95P), 99th percentile (RI99P) for the period 1971–2005. The increasing and decreasing trends are denoted by upward and downward triangles, respectively. The interpolated values of the trend magnitudes are shown.

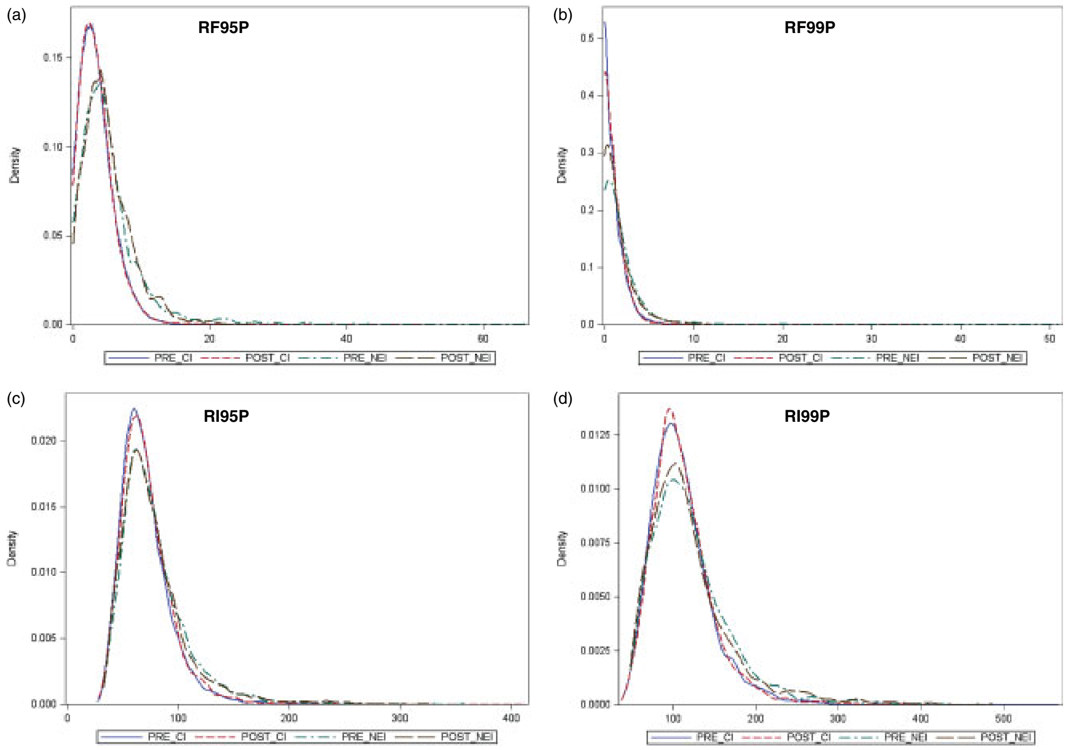

Figure 9. Probability density function (PDF) of monsoon rainfall for (a) frequency of exceedance of the 95th percentile (RF95P), (b) 99th percentile (RF99P), and for (c) intensity of exceedance of the 95th percentile (RI95P), (d) 99th percentile (RI99P) for the pre-1990 period (1971–1989) in central India (PRE_CI) and northeast India (PRE_NEI) and for the post-1990 period (1990–2005) in central India (POST_CI) and northeast India (POST_NEI).

© 2014 Royal Meteorological Society

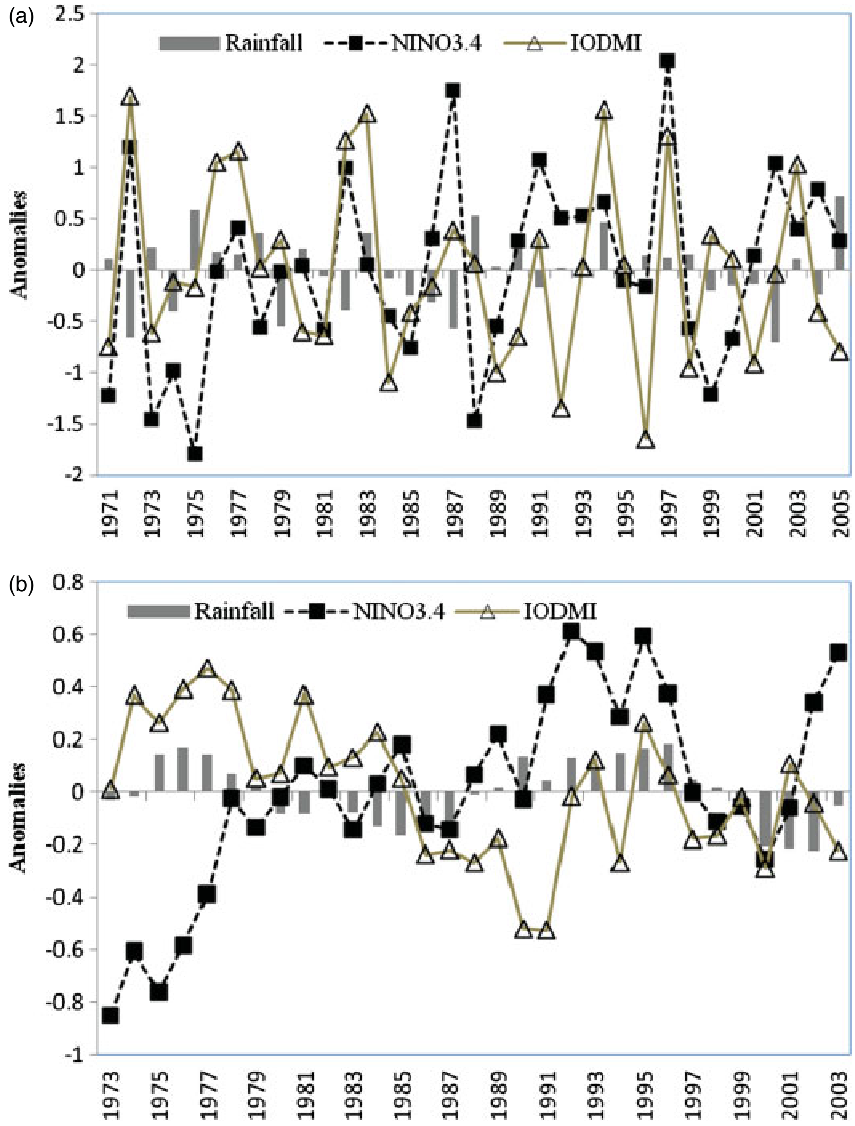

Figure 10. Time series of (a) the normalized anomalies of all India monsoon rainfall, NINO3.4 and IODMI in the monsoon season (June to September) and (b) the 5-year average of the normalized anomalies of same variables.

the eastern pole of IODMI and R100 aggregated over the central region for the same period, but not for the period 1971–2005. This suggests that the influence of IOD on extreme rainfall is very sensitive to the study period.

5. Discussion and conclusion

Results of this study provide several interesting features about the changing characteristics of monsoon rainfall for the period 1971–2005. First, the study period is characterized by a large interannual variability, leading to the identification of more nonsignificant trends in most of the rainfall indices. The second important feature is the lack of large scale spatial uniformity in terms of the presence of both the increasing and decreasing trends. Not for the Indian climate only, this has been reported for several countries that the signals of change in rainfall extremes are spatially less consistent in contrast to an apparent change in temperature extremes (Malhi and Wright, 2003; Zhang *et al.*, 2005). In general, the hypothesis suggests that global warming-induced accelerated hydrological cycle intensifies the interannual variability (Richard *et al.*, 2012). For both the south Asian and Indian monsoon system, simulation studies have also indicated an increased interannual variability in terms of extreme dry and wet rainfall events primarily because of warming (Meehl and Arblaster, 2003; May, 2011). Under this circumstance where interannual variability is sufficiently large compare to the significance of the trends, as suggested by Nicholls (2001) and followed by many other research studies (Moberg and Jones 2005), more information can be gained through explaining the congregation of trend magnitudes at the subregional or even at smaller spatial scale.

The result that stands out in this analysis is the clear increases in dry spells and moisture stress situation as

© 2014 Royal Meteorological Society

Table 5. Summary of the partial correlation of rainfall indices with the ENSO and IOD indices showing the frequency of significant increasing and decreasing trends at the $\alpha = 0.05$ and 0.1 levels from the total of 1240 grids.

Rainfall indices	ENSO/IOD indices	Positive correlation			Negative correlation		
		Total	$\alpha = 0.05$	$\alpha = 0.1$	Total	$\alpha = 0.05$	$\alpha = 0.1$
PRCPTOT	NINO3.4	322	9	21	918	158	267
	IODMI	660	36	83	580	18	42
Wet days	NINO3.4	172	2	3	1068	405	540
	IODMI	794	62	131	446	12	38
SDII	NINO3.4	634	45	88	606	54	89
	IODMI	508	25	39	732	46	87
RM	NINO3.4	215	3	15	1025	302	433
	IODMI	746	85	137	494	16	42
CDD	NINO3.4	1003	159	262	237	8	18
	IODMI	453	14	26	787	28	74
AII	NINO3.4	198	2	9	1042	354	491
	IODMI	836	74	152	404	6	29
RX1D	NINO3.4	613	32	71	627	54	87
	IODMI	495	19	31	745	54	109
R100	NINO3.4	623	18	61	545	41	80
	IODMI	503	32	52	665	43	81
R99P	NINO3.4	707	70	106	533	25	50
	IODMI	461	17	26	779	47	90
RF99p	NINO3.4	624	23	46	616	60	93
	IODMI	533	24	47	707	25	79
RI99p	NINO3.4	599	51	77	641	64	90
	IODMI	541	20	42	699	53	97

evident from the significance of the trends in CDD and AII along with their spatial coherence. Although this is consistent with the increases in drought conditions in the tropical countries since the 1970s (Trenberth *et al.*, 2007), analysis of the global datasets, however, showed a tendency towards wetter condition, with a general decrease in CDD (Frich *et al.*, 2002; Alexander *et al.*, 2006). Note that the drying signals in terms of increased CDD and decreased wet days and RM are observed in large parts of the country in the active monsoon months of July and August (Tables 2 and 3; and Figure 4) in contrast to a relatively wetting tendency in June and September. In particular, the drying tendency in July, occurred mostly during El Niño events since the 1960s, has socio-economic relevance, as they cause in large scale droughts all over India (Ihara *et al.*, 2008). It is important to point that the contrasting characteristics have not been captured in the monsoon scale analysis and thus, underscore the sensitivity of monsoon rainfall to the subseasonal analysis. Furthermore, the drying rainfall tendency is reflected through the relative spatial dominance of the decreasing patterns in wet days and moderate rainfall frequency (Figure 2). The PDFs indicates that the drying tendency has increased noticeably since the 1990s, which mark the start of the warmest decade (Folland *et al.*, 2001).

Most of the wet extreme indices (RX1D, R100, R95p, R99p, RF95p, RF99p, RI95p and RI99p) show a general increase during the rapid warming period over large parts of the country, although there is difference in the proportion of trends along with their spatial coverage with respect to the indices (Table 4; and Figures 6 and 8). For the indices with higher percentile threshold, the increasing trends are spatially more consistent. While the elongated right tail of the PDFs suggests a general occurrence of the extreme events during the warming era irrespective of the subperiods and regions, the frequency of the extremes appears to have increased marginally since the 1990s as evident from the positive swing in the PDFs. Since the total rainfall index (PRECTOT) has not depicted the observed changes in the extreme characteristics, it appears that the increases in extreme rainfall indices might offset partially the decreases in moderate rainfall (RM) (Trenberth *et al.*, 2003), although their relative contribution to the monsoon total differs. The other noteworthy outcome is the increase in variability in both spatial and temporal context; since the opposite aspects of rainfall do not occur at a particular time and location, one dominates over the other in terms of drought or flood. A critical visual comparison also reveals that there are certain patches in the southeast and elevated parts of the peninsular and the northwestern Himalaya where increases in PRECTOT are associated with a conspicuous rise in both the wet days and extreme rainfall indices. Similar to our results, the adjacent country China has also experienced significant decreases in wet days, with a mixture of increases and decreases in PRECTOT and increases in rainfall intensity (Zhai *et al.*, 2005).

It is clear from these results that the monsoon rainfall of India during the period 1971–2005 is already changing in line with predicted changes for the future

© 2014 Royal Meteorological Society

(a) NINO3.4 correlation

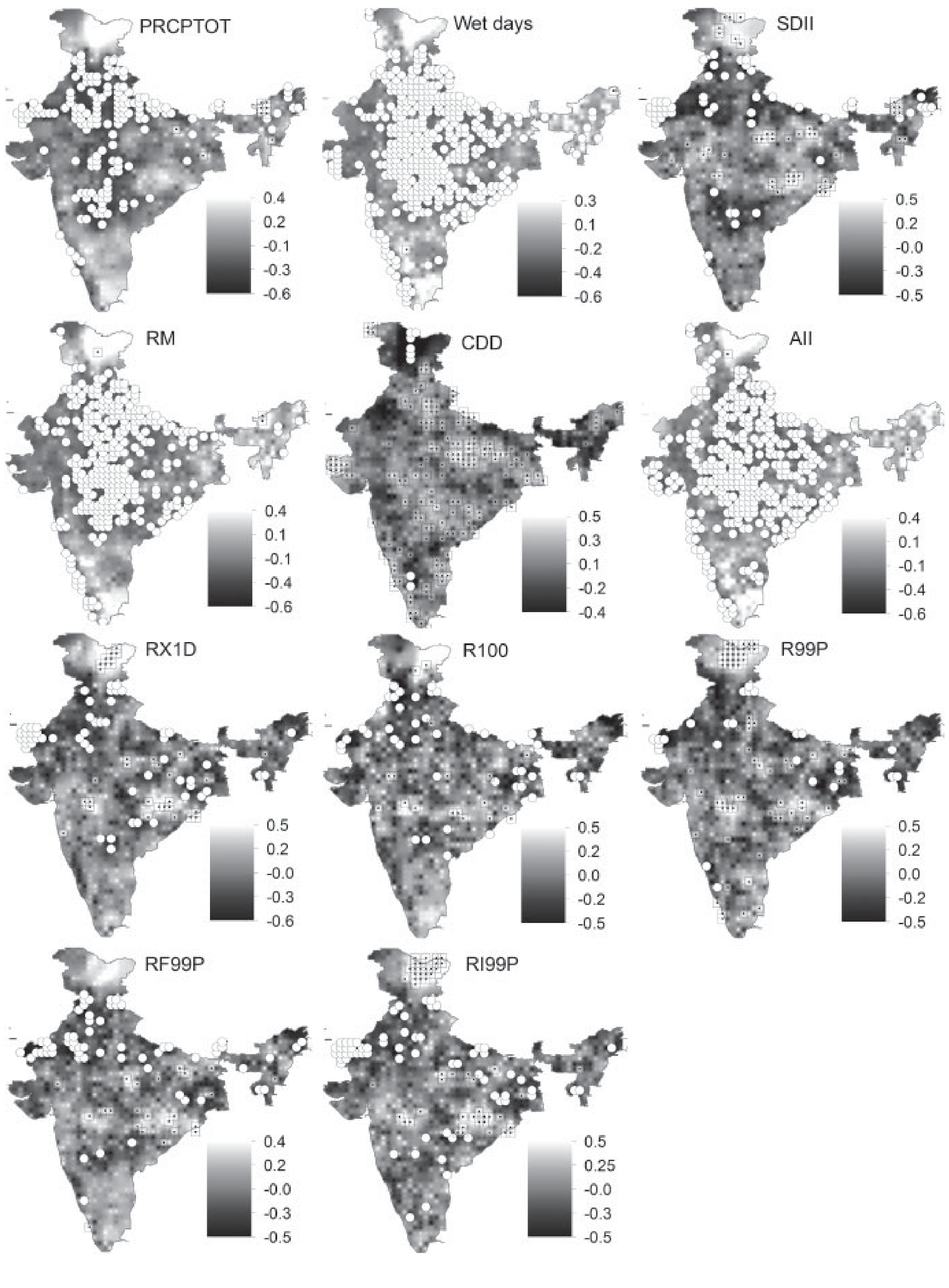

Figure 11. Spatial distribution of the partial correlation of rainfall indices with (a) the ENSO index NINO3.4, excluding the influence of the IOD index IODMI, and with (b) the IOD index IODMI, excluding the influence of the ENSO index NINO3.4. Circles indicate the negative correlation and square with dots denote the positive correlation significant at the $\alpha = 0.05$ level.

(Ashfaq *et al.*, 2009; May, 2011). Although we find that the rainfall trend and variability is partly explained by the large scale phenomenon ENSO and IOD, the forcing mechanism of the synoptic scale disturbances (Ajayamohan *et al.*, 2010) and the regional land-use changes (e.g. urbanization, Kishtawal *et al.*, 2009) may have influenced the observed trends. However, analysis of a high resolution dataset using robust statistical tools provides the spatial details of the trends and their linkages. The observed changes in monsoon rainfall have already impacted the social and economic aspects of the country (Mall *et al.*, 2006). In particular, the emergence

© 2014 Royal Meteorological Society

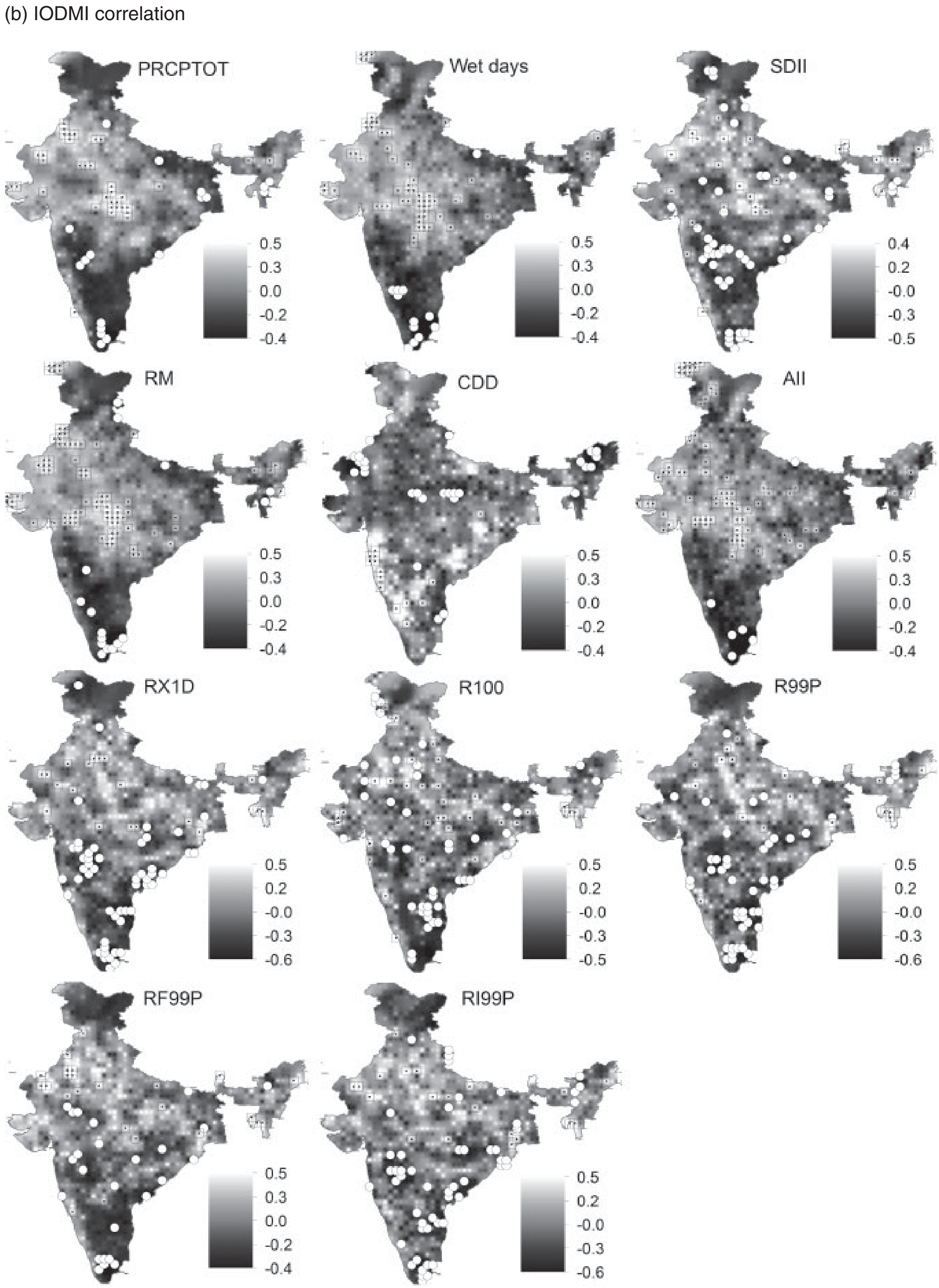

Figure 11. Continued

of dry spells over the agriculturally dominant central and north India could affect the food production of the country. Since the El Niño events can be predicted well in advance, the spatially consistent linkages of the NINO3.4 index with the drought indices (CDD and AII) can be used to implement drought adaptation strategies. In the context of the rising population and water scarcity in India, future research is needed to understand the regional driver of changes to meet the developmental goals at ecosystem scale.

Acknowledgements

We thank all the anonymous reviewers and the editor of the journal for valuable suggestions that helped to improve the quality of this article. This work was

© 2014 Royal Meteorological Society

supported by the Indian Council of Agricultural Research (ICAR), New Delhi. We also thank the Indian Meteorological Department, Pune, for providing the daily gridded dataset for this research.

References

Ajayamohan RS, Rao SA. 2008. Indian ocean dipole modulates the number of extreme rainfall events over India in a warming environment. *J. Meteorol. Soc. Jpn.* **86**: 245–252.

Ajayamohan RS, Merryfield WJ, Kharin VV. 2010. Increasing trend of synoptic activity and its relationship with extreme rain events over central India. *J. Clim.* **23**: 1004–1013.

Alexander LV, Zhang X, Peterson TC, Caesar J, Gleason B, Klein Tank AMG, Haylock M, Collins D, Trewin B, Rahimzdeh F, Tagipour A, Kumar Kolli R, Revadekar JV, Griffiths G, Vincent L, Stephenson DB, Burn J, Aguilar E, Brunet M, Taylor M, New M, Zhai P, Rusticucci M, Vazquez Aguirre JL. 2006. Global observed changes in daily climate extremes of temperature and precipitation. *J. Geophys. Res.* **111**: D05109, DOI: 10.1029/2005JD006290.

Annamalai H, Xie SP, McCreary JP, Murtugudde R. 2005. Impact of Indian ocean sea surface temperature on developing El Niño*. *J. Clim.* **18**: 302–319.

Ashfaq M, Shi Y, W-wen T, Trapp RJ, Gao X, Pal JS, Diffenbaugh NS. 2009. Suppression of south Asian summer monsoon precipitation in the 21st century. *Geophys. Res. Lett.* **36**: L01704, DOI: 10.1029/2008GL036500.

Ashok K, Guan Z, Yamagata T. 2001. Impact of the Indian Ocean dipole on the relationship between the Indian monsoon rainfall and ENSO. *Geophys. Res. Lett.* **28**: 4499–4502.

Ashok K, Chan W-L, Motoi T, Yamagata T. 2004. Decadal variability of the Indian Ocean Dipole. *Geophys. Res. Lett.* **31**: L24207, DOI: 10.1029/2004GL021345.

Ashok K, Saji NH. 2007. On the impacts of ENSO and Indian Ocean dipole events on sub-regional Indian summer monsoon rainfall. *Nat. Hazards* **42**: 275–283.

Bainnes PG, Folland CK. 2007. Evidence for a rapid climate shift across the late 1960s. *J. Clim.* **20**: 2721–2744.

Behera SK, Krishnan R, Yamagata T. 1999. Unusual ocean–atmosphere conditions in the tropical Indian Ocean during 1994. *Geophys. Res. Lett.* **26**: 3001–3004.

Boschat G, Terray P, Masson S. 2012. Robustness of SST teleconnections and precursory patterns associated with the Indian summer monsoon. *Clim. Dynam.* **38**: 2143–2165.

Carvalho LMV, Jones C, Silva AE, Liebmann B, Silva PL. 2010. The South American Monsoon System and the 1970s climate transition. *Int. J. Climatol.* **31**: 1248–1256, DOI: 10.1002/joc.2147.

Costa AC, Soares A. 2009. Trends in extreme precipitation indices derived from a daily rainfall database for the South of Portugal. *Int. J. Climatol.* **29**: 1956–1975.

Das PK, Chakraborty A, Seshasai MVR. 2013. Spatial analysis of temporal trend of rainfall and rainy days during the Indian Summer Monsoon season using daily gridded ($0.5^\circ \times 0.5^\circ$) rainfall data for the period of 1971–2005. *Meteorol. Appl.*, DOI: 10.1002/met.1361.

Duncan JMA, Dash J, Atkinson PM. 2013. Analysing temporal trends in the Indian Summer Monsoon and its variability at a fine spatial resolution. *Clim. Change* **117**: 119–131.

Folland CK, Karl TR, Christy JR, Clarke RA, Gruza GV, Jouzel J, Mann ME, Oerlemans J, Salinger MJ, Wang S-W. 2001. Observed climate variability and change. In Climate change 2001: The Scientific Basis, *Contribution of Working Group 1 to the Third Assessment Report of the Intergovernmental Panel on Climate Change*, Houghton JT, Ding Y, Griggs DJ, Noguer M, van der Linden PJ, Dai X, Maskell K, Johnson CA (eds). Cambridge University Press: Cambridge, UK; 99–182.

Frich P, Alexander LV, Della-Marta P, Gleason B, Haylock M, Klein Tank AMG, Peterson T. 2002. Observed coherent changes in climatic extremes during the second half of the twentieth century. *Clim. Res.* **19**: 193–212.

Gadgil S, Vinayachandran PN, Francis PA. 2003. Droughts of the Indian summer monsoon: role of clouds over the Indian Ocean. *Curr. Sci.* **85**: 1713–1719.

Ghosh S, Das D, Kao S-C, Ganguly AR. 2012. Lack of uniform trends but increasing spatial variability in observed Indian rainfall extremes. *Nat. Clim. Change* **2**: 86–91.

Goswami BB, Mukhopadhyay P, Mahanta R, Goswami BN. 2010. Multiscale interaction with topography and extreme rainfall events in the northeast Indian region. *J. Geophys. Res.* **115**: D12114, DOI: 10.1029/2009JD012275.

Goswami BN, Venugopal V, Sengupta D, Madhusoodanan MS, Xavier PK. 2006. Increasing trend of extreme rain events over India in a warming environment. *Science* **314**: 1442–1445.

Griffiths ML, Bradley RS. 2007. Variations of twentieth-century temperature and precipitation extreme indicators in the Northeast United States. *J. Clim.* **20**: 5401–5417.

Hartkamp AD, De Beurs K, Stein A, White JW. 1999. *Interpolation Techniques for Climate Variables, NRG-GIS Series 99–01*. CIMMYT: Mexico, DF.

Haylock M, Nicholls N. 2000. Trends in extreme rainfall indices for an updated high quality data set for Australia, 1910–1998. *Int. J. Climatol.* **20**: 1533–1541.

Hirsch RM, Slack JR, Smith RA. 1982. Techniques for trend analysis for monthly water quality data. *Water Resour. Res.* **18**: 107–121.

Hisdal H, Stahl K, Tallaksen LM, Demuth S. 2001. Have streamflow droughts in Europe become more severe or frequent. *Int. J. Climatol.* **21**: 317–333.

Houghton JT, Ding Y, Griggs DJ, Noguer M, van der Linden PJ, Dai X, Maskell K, Johnson CA (eds). 2001. *Climate Change 2001: the scientific basis, Contribution of Working Group 1 to the Third Assessment Report of the Intergovernmental Panel on Climate Change*. Cambridge University Press: Cambridge, UK; 881.

Ihara C, Kushnir Y, Cane MA. 2008. July droughts over homogeneous Indian monsoon region and Indian Ocean dipole during El Niño events. *Int. J. Climatol.* **28**: 1799–1805.

Katz RW. 1985. Probabilistic models. In *Probability, Statistics, and Decision Making in the Atmospheric Sciences*, Murphy AH, Katz RW (eds). Westview; 261–288.

Kiktev D, Sexton D, Alexander L, Folland C. 2003. Comparison of modelled and observed trends in indices of daily climate extremes. *J. Clim.* **16**: 3560–3571.

Kishtawal CM, Niyogi D, Tewari M, Pielke RAS, Shepherd JM. 2009. Urbanization signature in the observed heavy rainfall climatology over India. *Int. J. Climatol.* **30**: 1908–1916.

Klein Tank AMG, Können GP. 2003. Trends in indices of daily temperature and precipitation extremes in Europe, 1946–99. *J. Clim.* **16**: 3665–3680.

Klein Tank AMG, Peterson TC, Quadir DA, Dorji S, Zou X, Tang H, Santhosh K, Joshi UR, Jaswal AK, Kolli RK, Sikder AB, Deshpande NR, Revadekar JV, Yeleuova K, Vandasheva S, Faleyeva M, Gomboluudev P, Budhathoki KP, Hussain A, Afzaal M, Chandrapala L, Anvar H, Amanmurad D, Asanova VS, Jones PD, New MG, Spektorman T. 2006. Changes in daily temperature and precipitation extremes in Central and South Asia. *J. Geophys. Res.* **111**: D16105 DOI: 10.1029/2005JD006316.

Klein Tank AMG, Zwiers FW, Xuebin Z. 2009. Guidelines on analysis of extremes in a changing climate in support of informed decisions for adaptation. In *World Meteorological Organisation*, Rep. Climate Data and Monitoring WCDMP-No. 72, WMO-TD No 1500, Geneva, Switzerland, 55 pp.

Krishna Kumar K, Rajagopalan B, Cane MA. 1999. On the weakening relationship between the Indian monsoon and ENSO. *Science* **287**: 2156–2159.

Krishnamurthy V, Shukla J. 2000. Intra-seasonal and inter-annual variability of rainfall over India. *J. Clim.* **13**: 4366–4377.

Krishnamurthy CKB, Lall U, Kwon H-H. 2009. Changing frequency and intensity of rainfall extremes over India from 1951 to 2003. *J. Clim.* **22**, DOI: 10.1175/2009JCLI2896.1.

Kucharski F, Bracco A, Yoo JH, Tompkins A, Feudale L, Ruti P, Dell' AA. 2009. A Gill-Mastuno-type mechanism explains the Tropical Atlantic influence on African and Indian Monsoon rainfall. *Quart. J. Royal. Meteoro. Soc.* **135**: 569–579.

Kumar KR, Sahai AK, Kumar KK, Patwardhan SK, Mishra PK, Revadekar JV, Kamala K, Pant GB. 2006. High-resolution climate change scenarios for India for the 21st century. *Curr. Sci.* **90**: 334–345.

Lau KM, Kim MK, Kim KM. 2006. Asian summer monsoon anomalies induced by aerosol direct forcing: the role of the Tibetan Plateau. *Clim. Dynam.* **26**: 855–864.

Lettenmaier DP, Wood EF, Wallis JR. 1994. Hydro-climatological trends in the continental United States, 1948–88. *J. Clim.* **7**: 586–607.

Mall RK, Singh R, Gupta A, Srinivasan G, Rathore LS. 2006. Impact of climate change on Indian agriculture: a review. *Clim. Change* **78**: 445–478.

© 2014 Royal Meteorological Society

Malhi Y, Wright J. 2003. Spatial patterns and recent trends in the climate of tropical rainforest regions. *Phil. Trans. R. Soc. Lond. B* **2004**: 359, DOI: 10.1098/rstb.2003.1433.

May W. 2011. The sensitivity of the Indian summer monsoon to a global warming of 2 °C with respect to pre-industrial times. *Clim. Dynam.* **37**: 1843–1868.

Meehl GA, Arblaster JM. 2003. Mechanisms for projected future changes in south Asian monsoon precipitation. *Clim. Dynam.* **21**: 659–675.

Moberg A, Jones PD. 2005. Trends in indices for extremes in daily temperature and precipitation in central and western Europe, 1901–99. *Int. J. Climatol.* **25**: 1149–1171.

Naidu CV, Durgalakshmi K, Muni Krishna K, Rao SR, Satyanarayana GC, Lakshminarayana P, Rao LM. 2009. Is summer monsoon rainfall decreasing over India in the global warming era? *J. Geophys. Res.* **114**: D24108, DOI: 10.1029/2008JD011288.

Nicholls N. 2001. The insignificance of significance testing. *Bull. Am. Meteorol. Soc.* **82**: 981–986.

Nigam S, Bollasina M. 2010. "Elevated heat pump" hypothesis for the aerosol-monsoon hydroclimate link: "Grounded" in observations? *J. Geophys. Res.* **115**: D16201, DOI: 10.1029/2009JD013800.

Panda DK, Kumar A, Singandhupe RB, Sahoo N. 2013. Hydroclimatic changes in a climate-sensitive tropical region. *Int. J. Climatol.* **33**: 1633–1645, DOI: 10.1002/joc.3538.

Pattnayak KC, Panda SK, Dash SK. 2013. Comparative study of regional rainfall characteristics simulated by RegCM3 and recorded by IMD. *Global Planet. Change* **106**: 111–122.

Rajeevan M, Bhate J, Jaswal A. 2008. Analysis of variability and trends of extreme rainfall events over India using 104 years of gridded daily rainfall data. *Geophys. Res. Lett.* **35**: L18707, DOI: 10.1029/2008GL035143.

Rajeevan M, Bhate J. 2009. A high resolution daily gridded rainfall dataset (1971–2005) for mesoscale meteorological studies. *Curr. Sci.* **96**: 558–562.

Richard S, Naik N, Vogel L. 2012. Does global warming cause intensified interannual hydroclimate variability? *J. Clim.* **25**: 3355–3372.

Saji NH, Goswami BN, Vinayachandran PN, Yamagata T. 1999. A dipole mode in the tropical Indian Ocean. *Nature* **401**: 360–363.

Sarkar S, Singh RP, Kafatos M. 2004. Further evidences for weakening relationship of Indian rainfall and ENSO over India. *Geophys. Res. Lett.* **31**: L24207, DOI: 10.1029/2004GL020259.

Sen Roy S, Balling RC. 2004. Trends in extreme daily precipitation indices in India. *Int. J. Climatol.* **24**: 457–466.

Sen PK. 1968. Estimates of the regression coefficient based on Kendall's tau. *J. Am. Stat. Assoc.* **63**: 1379–1389.

Smith TM, Reynolds RW, Peterson TC, Lawrimore J. 2008. Improvements to NOAA's historical merged land-ocean surface temperature analysis (1880–2006). *J. Clim.* **21**: 2283–2296.

Srinivas CV, Hariprasad D, Bhaskar Rao DV, Anjaneyulu Y, Baskaran R, Venkatraman B. 2013. Simulation of the Indian summer monsoon regional climate using advanced research WRF model. *Int. J. Climatol.* **33**: 1195–1210, DOI: 10.1002/joc.3505.

Taschetto AS, Sen Gupta A, Hendon HH, Ummenhofer CC, England MH. 2011. The contribution of Indian Ocean sea surface temperature anomalies on Australian summer rainfall during El Nino events. *J. Clim.* **24**(14): 3734–3747.

Trenberth KE, Dai A, Rasmussen RM, Parsons DB. 2003. The changing character of precipitation. *Bull. Am. Meteorol. Soc.* **84**: 1205–1217.

Trenberth KE, Jones PD, Ambenje P, Bojariu R, Easterling D, Klein Tank A, Parker D, Rahimzadeh F, Renwick JA, Rusticucci M, Soden B, Zhai P. 2007. Observations: surface and atmospheric climate change. In Climate Change 2007: The Physical Science Basis, Contribution of Working Group I to the Fourth Assessment Report of the Intergovernmental Panel on Climate Change, Solomon S, Quin D, Manning M, Chen Z, Marquis M, Averyt KB, Tignor M, Miller HL (eds). Cambridge University Press: Cambridge, UK.

Vincent LA, Mekis É. 2006. Changes in daily and extreme temperature and precipitation indices for Canada over the twentieth century. *Atmosphere–Ocean* **44**: 177–193.

Webster PJ, Magańa VO, Palmer TN, Shukla J, Tomas RA, Yanai M, Yasunari T. 1998. Monsoons: processes, predictability and the prospects for prediction. *J. Geophys. Res.* **103**: 14451–14510.

Yatagai A, Kamiguchi K, Arakawa O, Hamada A, Yasutomi N, Kitoh A. 2012. APHRODITE: constructing a long-term daily gridded precipitation dataset for Asia based on a dense network of rain gauges. *Bull. Am. Meteorol. Soc.* **93**: 1401–1415.

Yue S, Wang CY. 2002. Regional streamflow trend detection with consideration of both temporal and spatial correlation. *Int. J. Climatol.* **22**: 933–946.

Zhai P, Zhang X, Wan H, Pan X. 2005. Trends in total precipitation and frequency of daily precipitation extremes over China. *J. Clim.* **18**: 1096–1108.

Zhang X, Harvey KD, Hogg WD, Yuzyk TR. 2001. Trends in Canadian streamflow. *Water Resour. Res.* **37**(4): 987–998.

Zhang X, Aguilar E, Sensoy S, Melkonyan H, Tagiyeva U, Ahmed N, Kutaladze N, Rahimzadeh F, Taghipour A, Hantosh TH, Albert P, Semawi M, Karam Ali M, Halal Said Al-Shabibi M, Al-Oulan Z, Zatari T, Al Dean Khelet I, Hammoud S, Demircan M, Eken M, Adiguzel M, Alexander L, Peterson T, Wallis T. 2005. Trends in middle east climate extremes indices during 1950–2003. *J. Geophys. Res.* **110**: 104, DOI: 10.1029/2005JD006181.

© 2014 Royal Meteorological Society